Inverse-photoemission study of unoccupied electronic states in Ge and Si: Bulk energy bands

D. Straub, L. Ley,* and F. J. Himpsel
IBM Thomas J. Watson Research Center, Box 218, Yorktown Heights, New York 10598
(Received 23 January 1985; revised manuscript received 21 August 1985)

We have measured **k**-resolved inverse-photoemission spectra of the Ge(111)2×1 and Si(111)2×1 surfaces. The main spectral features are well described in terms of direct transitions to the three lowest conduction bands along ΓL and a transition to a surface resonance near the conduction-band minimum via a surface umklapp process. An extra feature reflects a maximum in the density of empty states. Several critical points are determined, e.g., for Ge, L_1 at 0.7 eV, L_3 at 4.2 eV, and L_2' at 7.9 eV and a higher L point at 11 eV, and for Si, L_1 at 2.4 eV and L_3 at 4.15 eV above the valence-band maximum. By comparing our inverse-photoemission results with those from photoemission and optical spectroscopy we find that the E_1 transition could be lowered by the electron-hole interaction by up to 0.15 eV for Ge and 0.5 eV for Si. A comparison with first-principles and empirical band calculations is made.

I. INTRODUCTION

Energy band dispersions are a fundamental way to describe the electronic structure of a crystalline solid by displaying the relation between the two quantum numbers, for energy and momentum, of an electron in a solid. Experimentally, energy bands can be observed by various methods, most notably angle-resolved photoemission[1] and by inverse photoemission.[2] These two methods are capable of simultaneously measuring energy and momentum. Photoemission can probe electronic states below the Fermi level E_F and above the vacuum level E_{vac}. The gap between E_F and E_{vac} is now made available by the recently developed technique of inverse photoemission.[3] We apply this technique to measure conduction bands of germanium and silicon.

The band structure of germanium has been extensively studied by a great number of optical spectroscopies.[4] From these measurements critical point energies of interband transitions have been determined with high accuracy for the most prominent transitions, such as E_1 at 2.111 eV or E_2 at 4.35 eV.[4] If these transition energies are combined with initial-state energies obtained from photoelectron spectra, the position of conduction-band states can, in principle, be inferred. Using this approach, Grobman, Eastman, and Freeouf[5] derived a band-structure scheme of germanium that covers all of the valence bands and the conduction bands up to ~15 eV above the fundamental gap. They used a nonrelativistic, nonlocal pseudopotential calculation with adjustable parameters to fit the valence-band states to a large body of angle-integrated photoelectron spectra excited with photon energies between 6.5 and 25 eV. Critical point energies so derived were generally in good agreement with earlier angle-integrated[6,7] and recent angle-resolved measurements.[8–11] Low-lying conduction states were positioned by adding optical transition energies to the valence-band states, and the energies of some higher lying critical points were inferred from a direct-transition analysis of the photoemission spectra as a function of photon energy.

The band structure of silicon has received a large amount of attention due to the important role of Si in semiconductor devices. A large body of optical and photoemission date exists for silicon. Unoccupied bands play a role in the transport properties (e.g., electron mobility) of ballistic electron devices. Recently we have reported the first band-structure measurement of unoccupied states with inverse photoemission.[2,12,13] Here we compare the Si data with the results obtained for Ge.

It is apparent that the reliability of the conduction-band energies from optical data depends on the correct location of interband transitions in **k** space — a task that does not always lead to an unambiguous assignment, as discussed in Ref. 5. An independent determination of the energies and dispersion of conduction bands by angle-resolved inverse photoemission is thus desirable and such measurements will be presented below for Si and Ge. The same arguments hold for the energy bands at the surface of Ge. In this case our knowledge is less complete. The band dispersion of occupied surface states of Ge(111)2×1 has been measured,[14–16] but with controversial results. We have performed the first inverse photoemission measurements of unoccupied surface states or surface resonances for this surface and will discuss them in detail in a subsequent paper.[17]

From a more fundamental point of view such measurements could shed light on the question of whether or not it is reasonable to interpret photoelectron spectra and optical excitations in terms of a common one-electron energy scheme. The valence-band structure of Grobman, Eastman, and Freeouf represents, strictly speaking, the dispersion of ionization energies that are measured in photoelectron spectroscopy. The conduction-band energies, on the other hand, are chosen such that energy differences between valence and conduction bands agree with optical excitation energies. In inverse photoemission, finally, we measure the energy $h\nu$ that is released in the form of a photon when an electron is deposited from an initial state E_i outside the crystal into a final unoccupied state with energy $E_f = E_i - h\nu$. E_f is thus the energy of an

electron-affinity level.

Ionization energies and electron affinities differ from one-electron term values calculated in the Hartree-Fock scheme, for example, by the response of the electrons not directly involved in the transitions. They relax towards the hole and screen it in the photoemission process, and they move away from the incoming electron in the inverse photoemission process. Compared with their respective one-electron values, the ionization potential is lowered and the electron affinity is increased (i.e., the affinity level moves down). Relaxation energies are difficult to calculate because they are many-body effects. There appears to be, however, a simple relationship between an optical excitation energy $E_{1,2}$ from state 1 to state 2, and the corresponding ionization potential E_1 and electron affinity E_2 (see Fig. 1). We can compare the optical excitation with the sum of the photoemission and inverse photoemission processes: First we remove an electron from level 1 to infinity at the expense of the ionization energy E_1. In the second process we add an electron from infinity to level 2, thereby gaining the energy E_2. The optical excitation energy $E_{1,2}$ is not exactly equal to E_1-E_2. The missing energy $E_x=(E_1-E_2)-E_{1,2}$ is caused by the interaction of electron and hole that are simultaneously present after the optical excitation. Thus, E_x is the binding energy of the exciton formed by the electron-hole pair.

Examples for excitonic energies E_x that surpass those normally encountered in optical spectra (~ 10 meV) are core-level state to empty surface or bulk-state transitions (core excitons) where E_x reaches values of several hundred meV.[18–21] Hanke and Sham recently found that the bulk E_1 transition in diamond[22] and silicon[23] shows a substantial enhancement in oscillator strength over its single-particle value (see also Ref. 24 and 25). The enhancement is accompanied by an excitonic lowering of the transition threshold by ~ 1.5 eV (C) and 0.2 eV (Si) without the formation of a bound exciton. This unusually large effect is due to a reduced screening of the Coulomb interaction between electrons and holes, owing to the rather localized nature of the E_1 transition. For Si a similar electron-hole effect of about 0.6 eV was calculated by Pickett and Wang.[25] In silicon, we estimated[13] an excitonic lowering $E_x=0.5$ eV for the E_1 transition in qualitative agreement with theory. A smaller but still measurable effect is expected in Ge.

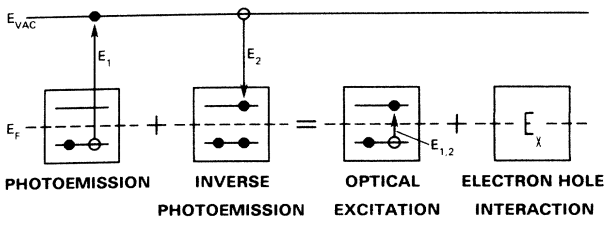

FIG. 1. Schematic representation of the relationship between photoelectron spectroscopy, inverse photoemission, and optical excitation involving levels 1 and 2 in a solid. In general, the optical excitation energy $E_{1,2}$ is smaller than the difference between the ionization energy E_1 and the electron affinity E_2 by an amount E_x which corresponds to the electron-hole interaction.

The paper is organized as follows. After a brief description of the apparatus and sample preparation in Sec. II we present the analysis of bulk features in the inverse photoemission spectra in Sec. III; first for Ge, then for Si. Thereby, we derive conduction-band dispersions along the Λ symmetry direction of the Brillouin zone. This is followed by a summary. In a subsequent publication (Ref. 17) we focus on surface-state transitions.

II. EXPERIMENTAL

The inverse photoemission spectra were recorded using a newly developed spectrometer which employs a fast ($f/4$) grating monochromator with simultaneous detection of photons with energies between 8 and 28 eV.[26] A parallel beam of electrons emitted from an electron gun with BaO cathode and Pierce-type geometry impinges onto the sample surface. Photons are detected at 45° from the sample normal with equal efficiency for both polarizations. The energy and momentum resolutions of the spectrometer are mainly limited by the thermal spread of the electrons, and amount to 0.3 eV and 0.1 Å^{-1}, respectively. Spectra are displayed by recording the energy distribution of the radiation that is emitted when electrons with a chosen initial energy E_i undergo radiative transition into conduction-band states with energies E_f. In the spectra to be discussed in the next section photon energies have been converted into final-state energies according to $E_f=E_i-h\nu$. The reference energy for E_i and E_f is the Fermi level E_F. Its position on the photon-energy scale was determined from the sharp high-energy cutoff in the spectrum of a thin Au film evaporated onto the semiconductor surface *in situ*.

The samples used were $3\times3\times20$-mm^3 bars of p-type Ge with a resistivity of 1.5 Ω cm. Our Si samples were of the same dimensions. We used n-type samples (As doped, $N_D=2.6\times10^{19}$ cm^{-3}) and p-type samples (B doped, $N_A=3\times10^{19}$ cm^{-3}), respectively. The heavy doping was chosen to reduce the voltage drop at the depletion layer, and the agreement in final-state energies for the two samples excludes charging or band bending as a source of systematic error in the measured band dispersions. A thin Al film sputtered onto the rear section of the Si and Ge bars after standard cleaning procedures provided an Ohmic contact to the sample holder as confirmed by I-V measurements.

These bars were cleaved in a vacuum of better than 1×10^{-10} torr along $[\bar{2}11]$ to expose (111) surfaces of high quality. The surface reconstruction was checked with low-energy electron diffiaction after the inverse photoemission spectra were taken so as to keep electron-beam-induced surface contamination to a minimum. The position of the Fermi level for the Ge(111)2×1 surface of p-type samples coincides[27,28] with the top of the valence band E_v to within 20 meV. We shall, therefore, assume $E_F-E_v=0$ for our analysis. For Si(111)2×1 we used $E_F-E_v=0.40$ eV (Ref. 29) for both p- and n-type samples.

III. RESULTS AND DISCUSSION

Figure 2 shows a series of inverse photoemission spectra obtained from a Ge(111)2×1 surface at normal elec-

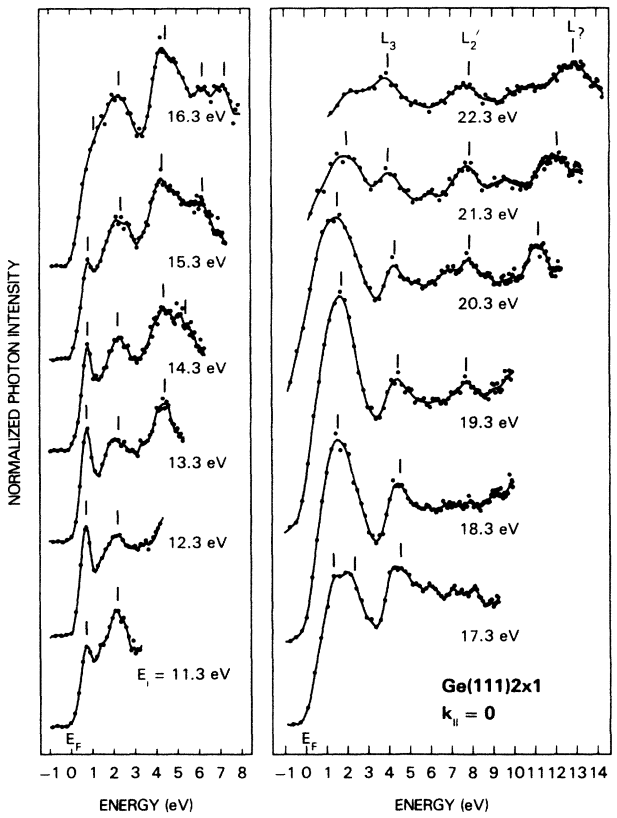

FIG. 2. Inverse photoemission spectra from the Ge(111)2×1 surface for normal electron incidence. Parameter is the energy of the electron beam, E_i, relative to the valence band maximum E_v. Transitions into various L critical points are marked in the 22.3-eV spectrum.

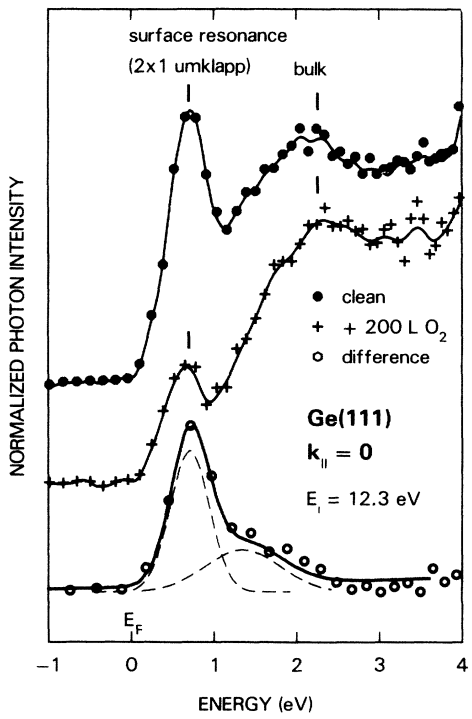

FIG. 3. Inverse photoemission spectra of Ge(111) for a clean 2×1 surface (solid circles, top panel) and after exposure to 200 L of oxygen (crosses, middle panel) ($1L = 10^{-6}$Torr sec). The lowest panel shows the difference spectrum indicating surface-resonance character of the peak at 0.7 eV above E_F and partial surface contribution on the low-energy shoulder of the 2.2-eV peak.

tron incidence and electron energies between 11.3 and 22.3 eV. In the following these data are analyzed in terms of surface and bulk interband transitions by methods similar to the ones used in angle-resolved photoemission (for a review see Ref. 1). We ascribe the sharp peak at 0.7 eV above E_F in Fig. 2 to transitions into an empty surface resonance since it disappears when the 2×1 reconstruction is destroyed by sample contamination (see Fig. 3). The remaining maxima in the spectra of Fig. 2 are stable with respect to contamination and are interpreted as transitions into bulk conduction-band states. The translational symmetry of the single-crystal surface ensures the conservation of $k_{||}$ (the electron momentum component parallel to the surface) in the radiative transitions that give rise to the structures of Fig. 2. For normal electron incidence and a nonreconstructed surface, $k_{||}$ vanishes and the transitions take place along the Λ symmetry direction, i.e., between Γ and L in the Brillouin zone (see Fig. 4). The momentum perpendicular to the surface, $k_\perp$, is scanned by tuning the photon energy, a unique capability of our apparatus.

Since the Si (111) and Ge (111) surfaces are reconstructed one has to take momentum transfer via the extra 2×1 surface reciprocal-lattice vector ($\mathbf{g}_{2\times1}$ in Fig. 4) into account. This process (often called a surface umklapp process) makes another line in $\mathbf{k}$ space accessible which passes through L and X (see Fig. 4). By testing the sensitivity of spectral features with respect to the 2×1 surface reconstruction we can decide between these two assignments.

In Fig. 5 we show in the left panel the nearly free-electron-like bands (dashed lines) together with a recently published band structure for the ΓL symmetry line[9] with the zero of energy placed at the valence-band maximum E_v. This band structure showed a good agreement with photoemission results along the ΓX direction.[9] However, there are other band-structure calculations available[10] that show a different band topology in the area of interest. This leaves us with some ambiguity in the assignment of calculated initial bands. Given this uncertainty, we have decided to use the nearly free-electron band as the dominant one (the so-called[30,31] "primary cone"). In this simple free-electron picture (dashed lines) only an inner potential of 8.8 eV below E_v (Ref. 32) and momentum transfer by bulk lattice vectors along the surface normal are taken into account. For the surface umklapp case we have to consider two such bands (see Fig. 5, right panel) corresponding to a transfer of $\pm\mathbf{g}_{2\times1}$. Without simplifications the ambiguity in assigning the spectral features to certain interband transitions would be prohibitive for interpreting the data. It is known from photoemission[33] and inverse photoemission[20] work on III-V compounds that the primary cone dominates but there exists significant emission from other bands. In cases where many initial-state bands contribute one probes final states at many $\mathbf{k}$ points and sees an averaged spectrum. The aver-

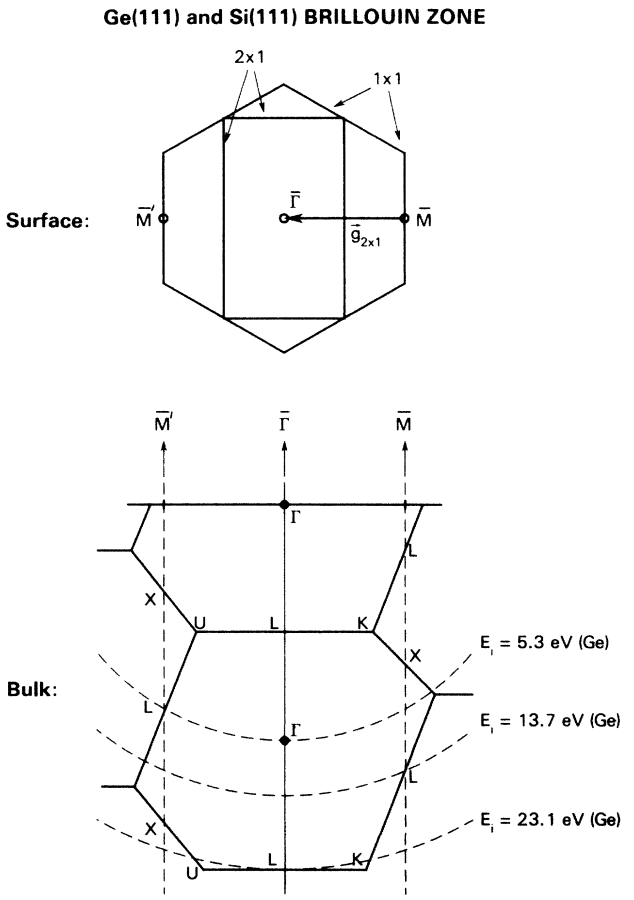

FIG. 4. Top panel: Surface Brillouin zone for the Si(111)- and Ge(111)2×1 surface. The extra surface reciprocal-lattice vector is marked $\mathbf{g}_{2\times1}$. The bottom panel shows a side view of the bulk Brillouin zone for Ge and Si. The dashed lines indicate the additional lines in $\mathbf{k}$ space through X and L which are accessible through the $\pm\mathbf{g}_{2\times1}$ surface umklapp process. Also indicated are the $\mathbf{k}$ points of the bulk Brillouin zone that are reached in the free-electron approximation for different initial electron energies E_i.

age reflects the one-dimensional density of states[34–36] along the line in $\mathbf{k}$ space that is accessible via momentum conservation. The unexplained stationary feature at 2.2 eV above E_v in our data is a candidate for a one-dimensional density-of-states peak near the maximum of the lowest Λ_1 band (see Fig. 6).

Most of the peaks in Fig. 2, however, can be attributed to direct interband transitions from the free-electron primary cone band into the lower conduction bands as shown in Fig. 6. From the experimentally obtained band dispersions, which cover almost 2/3 of the ΓL direction, various L critical points can be inferred. We find L_3 at 4.2 eV, L_2' at 7.9 eV, and a higher L point around 11 eV. From the transitions involving a surface umklapp process, we can deduce the L_1 point at 0.7 eV above E_v. The choice of one of the two possible initial bands in the right panel of Fig. 6 is consistent with the slight upwards dispersion that is observed with increasing photon energy. The other initial band would give a downward dispersion. However, weaker contributions from the second initial band are pos-

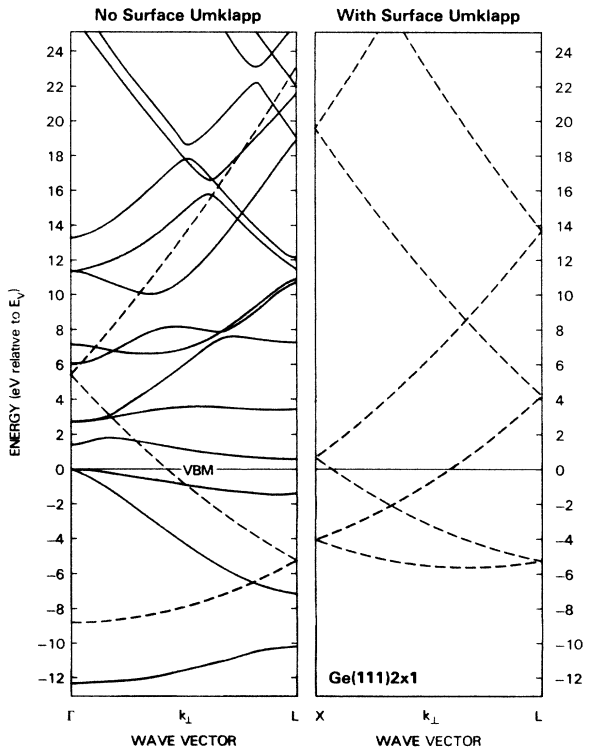

FIG. 5. Conduction-band structure of Ge along the ΓL direction and along the XLX direction with an additional $\mathbf{g}_{2\times1}$ umklapp process. The solid lines show an empirical pseudopotential calculation by Nelson *et al.* (Ref. 9); the dashed lines are free-electron-like bands calculated for an inner potential of $E_v - E_0 = 8.8$ eV.

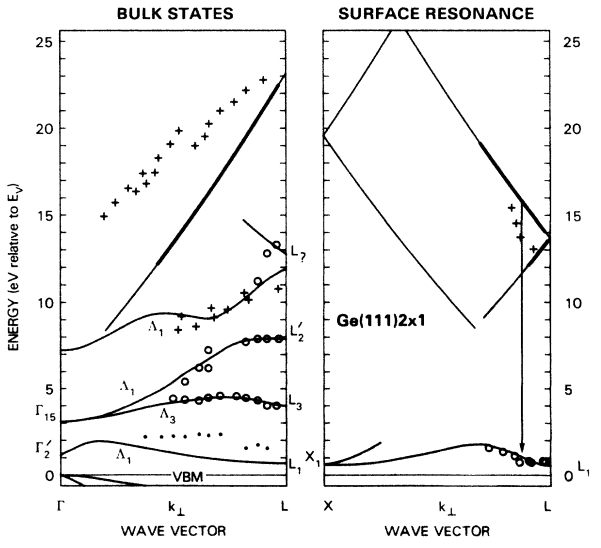

FIG. 6. Experimental conduction-band structure of Ge along the ΓL direction and along the XLX direction with an additional $\mathbf{g}_{2\times1}$ umklapp process. The dispersion of the three lowest conduction bands measured with inverse photoemission is indicated by open circles. Small closed circles denote a density-of-states feature. The crosses are results of a photoemission analysis in Ref. 10.

sible and, indeed, a second structure due to surface umklapp processes can be made out in the difference spectrum in Fig. 3. The crosses in Fig. 6 are taken from a recent photoemission study.[10] The agreement with our data is satisfactory. The surface umklapp process is seen in photoemission with the same upper band as in inverse photoemission. We note, however, that along ΓL the primary cone band seen in photoemission (Fig. 6, with crosses) corresponds to a higher band than the free-electron primary cone in inverse photoemission (Fig. 6, thick band without symbols).

With regard to the excitonic effects in Ge, we notice that the data points track the calculations[5,9,10] well, but are set off on the average by 0.15 ± 0.10 eV towards higher energy. In the calculation of Grobman *et al.*[5], the position of the L_1 critical point is matched to the $\bar{E}_1$ optical transition at 2.32 ± 0.02 eV which connects the topmost valence band with the lowest conduction band in the neighborhood of $\mathbf{k}=(2\pi/a)(\frac{1}{4},\frac{1}{4},\frac{1}{4})$.[37] The energy of the topmost valence band, in turn, is fixed at Γ and L by the photoemission data so that the discrepancy observed here could be interpreted as an excitonic lowering of the E_1 transition by $\Delta E_1=0.15$ eV analogous to the situation found in silicon.[13] The accuracy of the photoemission data used to determine the L_3' point is, however, limited to about 0.1 eV so that the significance of ΔE_1 is only marginal and within the combined error of our data (±0.1 eV) and the photoemission results.[10] Excitonic effects in the vicinity of the E_1 transition have been reported in the literature.[38–40] A sharp drop off of $\epsilon_2(\omega)$, the imaginary part of the dielectric constant above E_1, is the most characteristic of these effects which can be described as the interference of a discrete two-dimensional exciton with a quasicontinuous background.[41,42] A final decision on the magnitude of ΔE_1 requires obviously more accurate measurements of the dispersion of the uppermost valence band in Ge. The higher L points are also only slightly higher in energy in inverse photoemission than inferred from optical transition energies and photoemission results. The excitonic energies E_x are on the order of 0.1 eV for Ge and therefore of the same order as the ones reported for GaAs (Ref. 20) and substantially smaller than in the case of silicon.[13] There is a reduction in electron-hole interactions when going down the group-IV column from diamond to silicon and germanium that concurs with the increasingly metallic character of the elements.

For Si(111)2×1 the normal-incidence spectra are similar to those for Ge(111)2×1. As shown in Figs. 7 and 8 there exists a sharp structure[13,43] near the conduction-band minimum that is sensitive to the surface reconstruction and, therefore, is interpreted as a surface resonance. The remaining structures are interpreted as bulk interband transitions (see also Ref. 13). The initial-state bands (Fig. 9) are assumed to be free-electron-like with an inner potential of 12.1 eV below E_v consistent with photoemission.[10,44–46] Independent of this assumption we determine the L_1 and L_3 critical points as extrema in the band dispersion. We find the L_1 critical point at 2.4 eV and the L_3 critical point at 4.15 eV. A detailed discussion of these bulk bands and the electron-hole interaction in Si an be found in Ref. 13. Using the same arguments as for

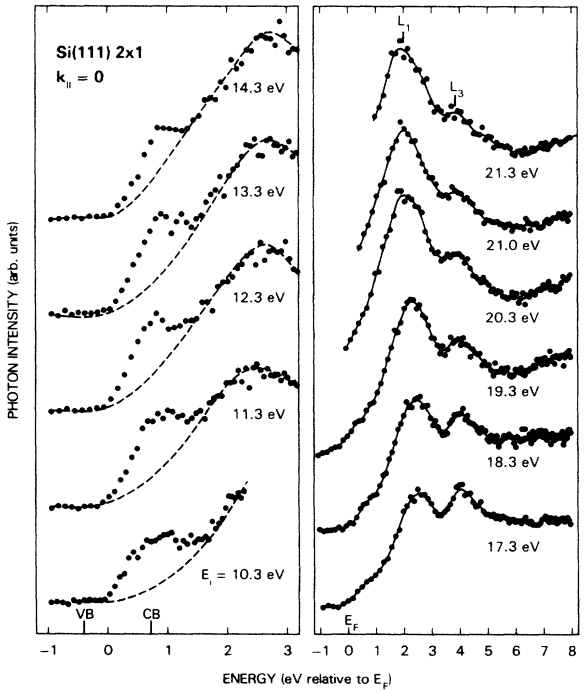

FIG. 7. Inverse photoemission spectra from the Si(111)2×1 surface for normal electron incidence. Parameter is the energy of the electron beam, E_i. The spectra show the low-E_f part for a limited range of initial energies between 10.3 and 14.3 eV. In the higher final-state energy spectra (right panel) the surface resonance at the conduction-band minimum is somewhat suppressed by contamination. VB marks the valence band maximum, CB the conduction band minimum.

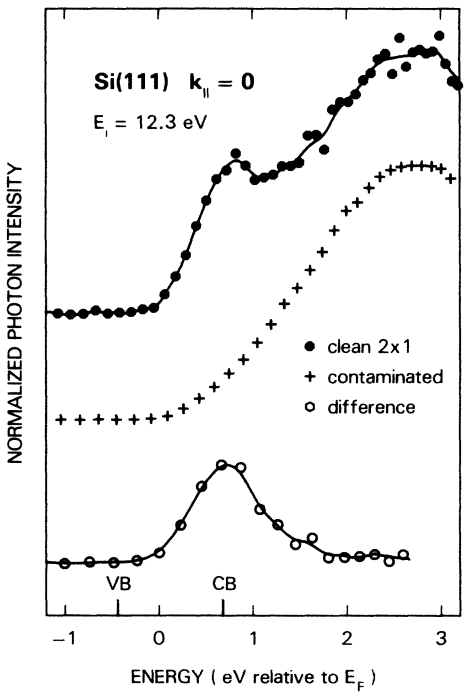

FIG. 8. Inverse photoemission spectra of Si(111) for a clean 2×1 surface (closed circles, top panel) and for a contaminated surface (crosses, middle panel). The lowest panel shows the difference spectrum indicating surface resonance character of the peak at 1.1 eV above E_v.

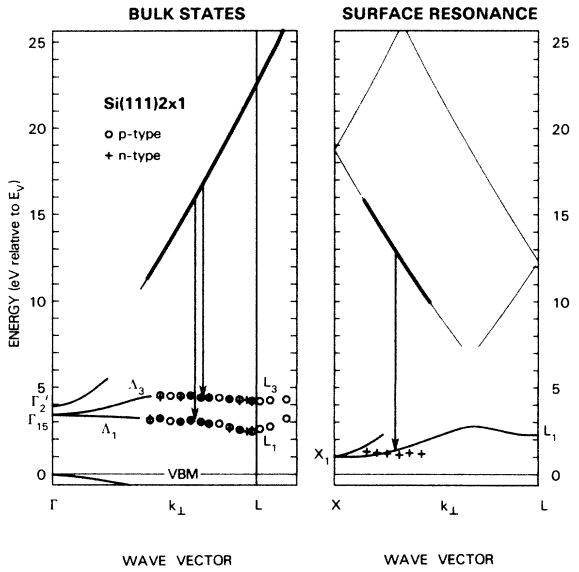

FIG. 9. Experiment conduction-band structure of Si along the ΓL direction and along the XLX direction with an additional $\mathbf{g}_{2\times1}$ umklapp process. The measured dispersion of the three lowest conduction bands is indicated by open circles for n-type and by crosses for p-type samples. The initial band is free-electron-like with an inner potential of $E_v - E_0 = 12.1$ eV.

Ge(111) we assign the contamination-sensitive surface resonance at 1.1 eV above E_v to transitions involving a $\mathbf{g}_{2\times1}$ surface umklapp process. In contrast with Ge, however, we are required to use the other initial band because the L_1 point lies much too high in Si to explain the surface umklapp peak. The different band topology of the lowest conduction band in Si (Γ_2' and Γ_{15} are reversed relative to Ge, different location of the conduction-band minima in $\mathbf{k}$ space) may justify the different assignment.

Our results on unoccupied bands in Ge and Si can be compared with numerous band calculations (Refs. 48–54 and Table I). The calculations are divided into two groups. Empirical methods[5,48] used previous experimental data as input and represent the state of our knowledge for the band structure of Ge and Si. We find small discrepancies between our data and these empirical bands for certain critical points (e.g., the L_1^c point in Si). These differences can be traced to the influence of the electron-hole interaction (discussed above) on the optical data which were used as an input for empirical calculations. For higher bands the empirical calculations suffer from insufficient experimental input. Our data provide the information that is needed for a more complete picture of the higher conduction bands. The second group of calculations are based on first-principles methods[50–54] (mostly the local-density theory). Although there exists substantial scatter among the results from different methods they all exhibit one common failure: They give conduction bands that are consistently too low compared with experiment. This discrepancy can be explained almost quantitatively by a well-known[55–59] problem with band calculations of semiconductors that use the local-density approximation. The band gap comes out only about half as large as measured. Since we have referenced the energies in Table I to the valence-band maximum we have to add half the band gap of Si ($E_g = 1.12$ eV) and Ge ($E_g = 0.66$ eV) to the calculated conduction-band values. This improves the agreement between theory and experiment to a degree which is comparable with the scatter between different calculations.

IV. SUMMARY AND CONCLUSIONS

The present investigation demonstrates the usefulness of $\mathbf{k}$-resolved inverse photoemission measurements to

TABLE I. Experimental and theoretical values of critical point energies for Si and Ge. Energies are given in eV relative to the valence band maximum E_v.

	Reference	Theory	Critical point L_3'	L_1	L_3	L_2'	$L_?$
Si sample							
Experiment	This work		−1.5[a]	2.4[b]	4.15		
Theory	Ref. 48	Empirical	−1.23	2.23	4.34		
	Ref. 51	First Principles	−1.40	1.46	3.66	7.73	
	Ref. 44	First Principles	−1.2	1.7	3.7	7.8	11.6
	Ref. 52	First Principles	−1.16	1.40	3.37		
	Ref. 53	First Principles	−1.13	1.58	3.92		
	Ref. 50	First Principles	−1.26	1.39	3.12		
	Ref. 54	First Principles	−1.16	1.36	3.55		
Ge sample							
Experiment	This work		−1.74[c]	0.7	4.2	7.9	11
Theory	Ref. 5	Empirical	−1.5	0.8	4.3	7.8	12.6
	Ref. 48	Empirical	−1.43	0.76	4.20		
	Ref. 51	First Principles	−1.40	0.52	3.80	7.77	
	Ref. 54	First Principles	−1.34	0.31	3.93		

[a]Average of the values reported in Refs. 45 and 47.
[b]A value of 2.2 eV was reported (Ref. 2) from inverse photoemission measurements on Si(111)7×7. This value is not as accurate as our result from Si(111)2×1 due to the momentum transfer via many extra surface lattice vectors on Si(111)7×7.
[c]Reference 10.

determine the dispersion of low-lying conduction states in semiconductors. We find that our data for bulk states are generally well reproduced by the empirical band structures that are fitted mainly to optical data. The small remaining differences can be traced to the Coulomb interaction between electron and hole in the optical transition. First-principles calculations using the local-density approximation need to be adjusted for the correct band gap to come to an agreement with the experiment.

ACKNOWLEDGMENT

L. L. thanks K. C. Pandey for a number of useful discussions. We thank A. Marx for his expert technical help.

*Permanent address: Max-Planck-Institut für Festkörperforschung, 7000 Stuttgart 80, West Germany.

[1]F. J. Himpsel, Adv. Phys. **32**, 1 (1983).

[2]F. J. Himpsel and T. Fauster, J. Vac. Sci. Technol. *A* **2**, 815 (1984).

[3]V. Dose, Prog. Surf. Sci. **13**, 225 (1983); N. V. Smith, Vacuum **33**, 803 (1983); F. J. Himpsel, Comments Solid State Phys. (to be published).

[4]See, for example, the recent compilation by L. Viña, S. Logothetidis, and M. Cardona, Phys. Rev. B **30**, 1979 (1984).

[5]W. D. Grobman, D. E. Eastman, and J. L. Freeouf, Phys. Rev. B **12**, 4405 (1975).

[6]L. Ley, S. P. Kowalczyk, R. Pollak, and D. A. Shirley, Phys. Rev. Lett. **29**, 1088 (1972).

[7]W. E. Spicer, J. Phys. (Paris) **34**, L6-19 (1973).

[8]R. D. Bringans and H. Höchst, Phys. Rev. B **25**, 1081 (1982).

[9]J. G. Nelson, W. J. Gignac, R. S. Williams, S. W. Robey, J. G. Tobin, and D. A. Shirley, Surf. Sci. **131**, 290 (1983).

[10]J. M. Nicholls, G. V. Hansson, U. O. Karlsson, P. E. S. Persson, R. I. G. Uhrberg, R. Engelhardt, S. A. Flodström, and E. E. Koch, Phys. Rev. B **32**, 6663 (1985).

[11]T. C. Hsieh, T. Miller, and T. C. Chiang, Phys. Rev. B **30**, 7005 (1984).

[12]F. J. Himpsel, Th. Fauster, and G. Hollinger, Surf. Sci. **132**, 22 (1983).

[13]D. Straub, L. Ley, and F. J. Himpsel, Phys. Rev. Lett. **54**, 142 (1985).

[14]J. M. Nicholls, G. V. Hansson, R. I. G. Uhrberg, and S. A. Flodström, Phys. Rev. B **27**, 2594 (1983).

[15]J. M. Nicholls, G. V. Hansson, U. O. Karlsson, R. I. G. Uhrberg, R. Engelhardt, K. Seki, S. A. Flodström, and E. E. Koch, Phys. Rev. Lett. **52**, 1555 (1984).

[16]F. Solal, G. Jezequel, A. Barsky, P. Steiner, R. Pinchaux, and Y. Petroff, Phys. Rev. Lett. **52**, 360 (1984).

[17]D. Straub, L. Ley, and F. J. Himpsel (unpublished).

[18]See, e.g., R. S. Bauer, R. Z. Bachrach, and J. C. McMenamin, Nuovo Cimento **39**, 409 (1977).

[19]D. Straub, M. Skibowski, and F. J. Himpsel, J. Vac. Sci. Technol. A3, 1484 (1985).

[20]D. Straub, M. Skibowski, and F. J. Himpsel, Phys. Rev. B **32**, 5237 (1985).

[21]For Ge we estimate an electron-hole interaction of about 0.2 eV for the Ge $3d$ core exciton at $h\nu=29.2$ eV. Thereby we assume that the surface optical transition [see D. E. Eastman and J. L. Freeouf, Phys. Rev. Lett. **33**, 1601 (1974)] has the shifted (Ref. 16) surface core level as initial state and the surface resonance (see Fig. 3) as final state.

[22]W. Hanke and L. Sham, Phys. Rev. B **12**, 4501 (1975).

[23]W. Hanke and L. Sham, Phys. Rev. Lett. **43**, 380 (1979); Phys. Rev. B **21**, 4656 (1980).

[24]M. del Castillo—Mussot and L. J. Sham, in *Proceedings of the 17th International Conference on the Physics of Semiconductors,* San Francisco, 1984, edited by J. D. Chadi and W. A. Harrison (Springer, New York, 1985), p. 1125.

[25]W. E. Pickett and C. S. Wang, Phys. Rev. B **30**, 4719 (1984).

[26]Th. Fauster, D. Straub, J. J. Donelon, D. Grimm, A. Marx, and F. J. Himpsel, Rev. Sci. Instrum. **56**, 1212 (1985).

[27]G. M. Guichar, G. A. Garry, and C. A. Sebenne, Surf. Sci. **85**, 326 (1979).

[28]G. W. Gobeli and F. G. Allen, Phys. Rev. **137**, A245 (1965).

[29]F. J. Himpsel, G. Hollinger, and R. A. Pollak, Phys. Rev. B **28**, 7014 (1983).

[30]G. D. Mahan, Phys. Rev. B 2, 4334 (1970).

[31]M. Cardona and L. Ley, in *Photoemission In Solids I,* Vol. 26 of *Topics in Applied Physics,* edited by M. Cardona and L. Ley (Springer, Berlin, 1978), p. 86.

[32]The inner potential of 8.8 eV was obtained by adjusting the free-electron-like bands to the final photoemission band reported in Ref. 9. Another value suggested from photoemission for E_0 is 7.7 eV in Ref. 10.

[33]G. P. Williams, F. Cerrina, J. Anderson, G. J. Lapeyre, R. J. Smith, J. Hermannson, and J. A. Knapp, Physica **117& 118B**, 350 (1983); G. P. Williams, F. Cerrina, G. J. Lapeyre, J. Anderson, R. J. Smith, and J. Hermanson, Phys. Rev. B (to be published).

[34]P. Thiry, R. Pinchaux, G. Marinez, Y. Petroff, J. Lecante, J. Paigne, Y. Ballu, C. Guillot, and O. Spanjaard, Solid State Commun. **27**, 99 (1978).

[35]K. A. Mills, O. Denley, P. Perfetti, and D. Shirley, Solid State Commun. **30**, 743 (1979).

[36]T. Grandke, L. Ley, and M. Cardona, Phys. Rev. B **18**, 3847 (1978).

[37]The E_1 transition is actually a doublet ($E_1=2.111$ eV and $E_1+\Delta_1=2.3$ eV; see Ref. 4) due to the spin-orbit splitting of the topmost valence band. The spin-orbit splitting is neglected in the calculation of Grobman *et al.* and they work with an average $\bar{E}_1$ which they take to be 2.32 eV. The spin-orbit splitting is not resolved in the photoemission data. Basing our analysis on the higher $\bar{E}_1$ value gives a conservative estimate for ΔE_1.

[38]M. Chandrasekhar and F. H. Pollak, Phys. Rev. B **15**, 2127 (1977).

[39]E. Schmidt, Phys. Status Solidi **B45**, K 39 (1971).

[40]D. T. F. Marple and H. Ehrenreich, Phys. Rev. Lett. **8**, 87 (1962).

[41]B. Velicky and J. Sak, Phys. Status Solidi **16**, 147 (1966).

[42]E. O. Kane, Phys. Rev. **180**, 852 (1969).

[43]B. Reihl *et al.* (unpublished).

[44]R. I. G. Uhrberg, G. V. Hansson, U. O. Karlsson, J. M. Nicholls, P. E. S. Persson, S. A. Flodström, R. Engelhardt, and E. E. Koch, Phys. Rev. B **31**, 3795 (1984).

[45]F. J. Himpsel, P. Heimann, and D. E. Eastman, Phys. Rev. B **24**, 2003 (1981): the L_3' energy was corrected for $E_F-E_v=0.40$ eV from Ref. 29.

[46]F. Houzay, G. M. Guichar, R. Pinchaux, P. Thiry, Y. Petroff, and D. Dagneaux, Surf. Sci. **99**, 28 (1980).
[47]R. I. G Uhrberg, G. V. Hansson, U. O. Karlsson, I. M. Nicholls, P. E. S. Persson, S. A. Flodström, R. Engelhardt, and E. E. Koch, Phys. Rev. Lett. **52**, 2265 (1984).
[48]J. R. Chelicowsky and M. L. Cohen, Phys. Rev. B **14**, 55 (1976).
[49]K. C. Pandey and J. C. Phillips, Phys. Rev. Lett. **32**, 1433 (1974).
[50]A. Zunger and M. L. Cohen, Phys. Rev. B **20**, 4082 (1979).
[51]C. S. Wang and B. M. Klein, Phys. Rev. B **24**, 3393 (1981).
[52]D. R. Hamann, Phys. Rev. Lett. **42**, 662 (1979).
[53]H. Stöhr and H. Bross, Phys. Status Solidi **B90**, 497 (1978).
[54]D. A. Papaconstantopoulos, Phys. Rev. B **27**, 2569 (1983).
[55]G. P. Kerker, Phys. Rev. B **24**, 3468 (1981).
[56]Z. H. Levine and S. G. Louie, Phys. Rev. B **25**, 6310 (1982).
[57]C. S. Wang and W. E. Pickett, Phys. Rev. Lett. **51**, 597 (1983).
[58]M. S. Hybertsen and S. G. Louie, Phys. Rev. Lett. **55**, 1418 (1985).
[59]W. E. Pickett, Comments Solid State Phys. **12**, 1 (1985).